



**HAL**  
open science

## Electromagnetic evidence for volatile-rich upwelling beneath the society hotspot, French Polynesia

Noriko Tada, Pascal Tarits, Kiyoshi Baba, Hisashi Utada, Takafumi Kasaya,  
Daisuke Suetsugu

► **To cite this version:**

Noriko Tada, Pascal Tarits, Kiyoshi Baba, Hisashi Utada, Takafumi Kasaya, et al.. Electromagnetic evidence for volatile-rich upwelling beneath the society hotspot, French Polynesia. *Geophysical Research Letters*, 2016, 43, pp.12,021-12,026. 10.1002/2016GL071331 . insu-03684934

**HAL Id: insu-03684934**

**<https://insu.hal.science/insu-03684934>**

Submitted on 1 Jun 2022

**HAL** is a multi-disciplinary open access archive for the deposit and dissemination of scientific research documents, whether they are published or not. The documents may come from teaching and research institutions in France or abroad, or from public or private research centers.

L'archive ouverte pluridisciplinaire **HAL**, est destinée au dépôt et à la diffusion de documents scientifiques de niveau recherche, publiés ou non, émanant des établissements d'enseignement et de recherche français ou étrangers, des laboratoires publics ou privés.

Copyright



## RESEARCH LETTER

10.1002/2016GL071331

## Key Points:

- Three-dimensional high electrical conductivity anomaly is imaged in the upper mantle beneath the Society hotspot
- The anomaly can be explained by the presence of upwelling of volatile-rich and partially molten material
- A pathway for ascending volatiles from the deeper part of the upper mantle has formed the Society hotspot

## Supporting Information:

- Supporting Information S1

## Correspondence to:

N. Tada,  
norikot@jamstec.go.jp

## Citation:

Tada, N., P. Tarits, K. Baba, H. Utada, T. Kasaya, and D. Suetsugu (2016), Electromagnetic evidence for volatile-rich upwelling beneath the society hotspot, French Polynesia, *Geophys. Res. Lett.*, 43, 12,021–12,026, doi:10.1002/2016GL071331.

Received 23 SEP 2016

Accepted 17 NOV 2016

Accepted article online 18 NOV 2016

Published online 3 DEC 2016

## Electromagnetic evidence for volatile-rich upwelling beneath the society hotspot, French Polynesia

Noriko Tada<sup>1</sup> , Pascal Tarits<sup>2</sup>, Kiyoshi Baba<sup>3</sup>, Hisashi Utada<sup>3</sup> , Takafumi Kasaya<sup>1</sup>, and Daisuke Suetsugu<sup>1</sup> 

<sup>1</sup>Japan Agency for Marine-Earth Science and Technology, Yokosuka, Japan, <sup>2</sup>UMR-Domaines Océaniques, Institut Universitaire Européen de la Mer, Plouzane, France, <sup>3</sup>Earthquake Research Institute, University of Tokyo, Tokyo, Japan

**Abstract** We have conducted a seafloor magnetotelluric survey that images, for the first time, three-dimensional electrical conductivity structure in the upper mantle beneath the Society hotspot. A striking feature in our model is a high-conductivity anomaly a few hundred kilometers in diameter, which is continuous from the lowest part of the upper mantle to a depth of approximately 50 km below sea level. Using theoretical and experimental results from mineral physics, we interpret the high-conductivity anomaly as evidence of the melt fraction up to 2.2 vol.%, which is robust regardless of assumed temperature, and the existence of carbonated silicate melt beneath the hotspot. Our results suggest that the Society hotspot is a pathway for ascending volatiles from the deeper part of the upper mantle to the surface.

### 1. Introduction

The South Pacific seafloor is characterized by a broadly elevated bathymetry and a concentration of volcanic island chains [Adam, 2005]. The Society hotspot is considered to be sourced from an upwelling from deep in the mantle that produced the island chain of the Society Islands [Aubaud *et al.*, 2005; Duncan and McDougall, 1976]. The topographic swell in the vicinity of the hotspot is attributed to the dynamic support of the ascending plume in the upper mantle beneath the hotspot [Adam *et al.*, 2010]. Previous seismic studies imaged a low-velocity anomaly beneath the hotspot [Suetsugu *et al.*, 2009]; however, because of the sparse observation array, the resolution of these images is insufficient to discuss the thermal and chemical properties of the plume.

Tomographic Investigation by seafloor ARray Experiment for the Society hotspot Project (hereinafter TIARES) was designed to image the possible plume with reasonable resolution using both magnetotelluric (MT) and seismological observations [Suetsugu *et al.*, 2012; Isse *et al.*, 2016]. We measured the natural time variations of the magnetic and electric fields in the period range of a few hundred seconds to approximately 1 day to probe the electrical conductivity structure of the upper mantle. The electrical conductivity of the mantle is sensitive to temperature, volatile (H<sub>2</sub>O and CO<sub>2</sub>) content, and the presence of melt [Sifré *et al.*, 2014], allowing quantitative constraints on the physical properties of the mantle beneath the hotspot.

### 2. Three-Dimensional Electrical Conductivity Image

#### 2.1. Analysis Procedures

We analyzed seafloor MT data from 20 sites around the Society hotspot, where the mean lithosphere age is approximately 70 Ma (Figure 1). Data for 11 of these sites were newly collected in the southeast of the Society hotspot through the TIARES project in 2008–2010 (Table S1) [Suetsugu *et al.*, 2012]; data for the other 9 sites were obtained in the vicinity and to the northwest of the hotspot in a previous study [Nolasco *et al.*, 1998]. The merged data set, along with a modern inversion technique [Baba *et al.*, 2013; Tada *et al.*, 2012] described below, enabled a 3-D electrical conductivity structure of the upper mantle to be constructed, whereas previous research obtained only a 2-D model, with limited discussion of the three-dimensionality of the structure [Nolasco *et al.*, 1998].

All time-series data of the electric and magnetic field variations were processed using the same robust methods to yield MT responses for each site [Chave and Thomson, 2004]. We estimated a regional 1-D conductivity profile that fits the averaged MT responses of all sites; this is termed the TIARES profile (Figure 2a). Three-dimensional inversion analysis was then carried out, applying the TIARES profile as the initial and prior

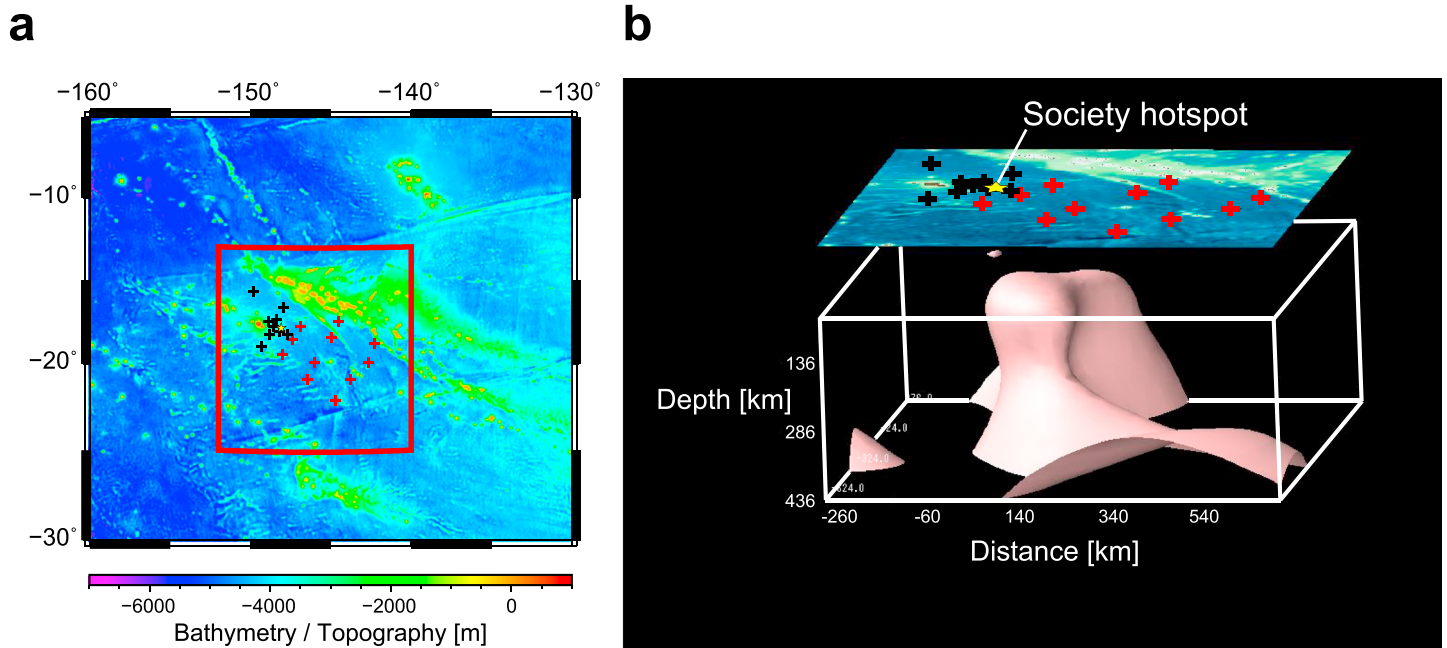


**Figure 1.** (a) Bathymetric map (ETOPO1, *Amente and Eakins*, 2009) and observation array. Yellow star indicates the location of the Society hotspot. Red and black crosses are the locations of the sites at which marine MT data were obtained newly [*Suetsugu et al.*, 2012] and previously [*Nolasco et al.*, 1998], respectively. Red square indicates the area shown in (b). (b) Three-dimensional electrical conductivity model obtained by an inversion of the MT data. The high-conductivity anomaly beneath the Society hotspot is depicted as the iso-surfaces of 0.3 S/m (pink). The origin of the horizontal directions is defined at the location of the Society hotspot. The bathymetric map is superimposed at the top.

models. The topographic and bathymetric effects on the MT responses were taken into consideration for both 1-D and 3-D analyses [*Baba and Chave*, 2005; *Baba et al.*, 2010; *Baba et al.*, 2013; *Tada et al.*, 2012], which is critical to obtain a reliable conductivity model. Details of the analysis conditions are provided in Text S1.

## 2.2. High Electrical Conductivity Anomaly

The 3-D inversion result shows a remarkably high-conductivity anomaly extending from the mantle transition zone to a depth of approximately 50 km below the sea surface (Figure 1). The tip of the most conductive ( $>0.3$  S/m) anomaly is located in the vicinity of the Society hotspot. This feature is well constrained by the data, because if the anomaly is trimmed, with all conductivities  $>0.035$  S/m set to this value, the RMS data misfit between the observed and modeled MT responses increases at the 95% confidence level (see Text S2).

Next, we discuss the differences between the high-conductivity anomaly (Zone A; Figure 2b) and the background area (the TIARES profile). We calculated the average conductivity weighted by the standard deviation as a function of depth for Zone A (Figure 2a). The mantle of Zone A is significantly more conductive than that of the TIARES profile at depths below  $\sim 70$  km. The contrast is almost two orders of magnitude, especially in the depth range 100–160 km. The 1-D conductivity profiles were also compared with those from two other areas, the Philippine Sea (PHS) and Western Pacific (PAC) [*Baba et al.*, 2010], which have seafloor ages of 10–70 and 150 Ma, respectively. The electrical conductivity of the TIARES profile is higher than that of PAC and lower than that of PHS at shallower ( $< \sim 220$  km) depths, but the three profiles are almost identical below 220 km. These features suggest that the TIARES profile is not anomalous in terms of age-dependence. However, the electrical conductivity for Zone A is unusually high ( $>0.1$  S/m) below  $\sim 120$  km depth, which is one to two orders of magnitude higher than the younger PHS profile.

## 3. Volatile Contents and Melt Fraction Calculation

We converted the estimated conductivity profiles for Zone A and the background area (TIARES) to temperature profiles assuming that the upper mantle consists only of dry olivine [*Gardés et al.*, 2014; Figure 3a]. The resulting temperature profile for Zone A exceeds the solidus of dry peridotite [*Aubaud et al.*, 2004] at depths

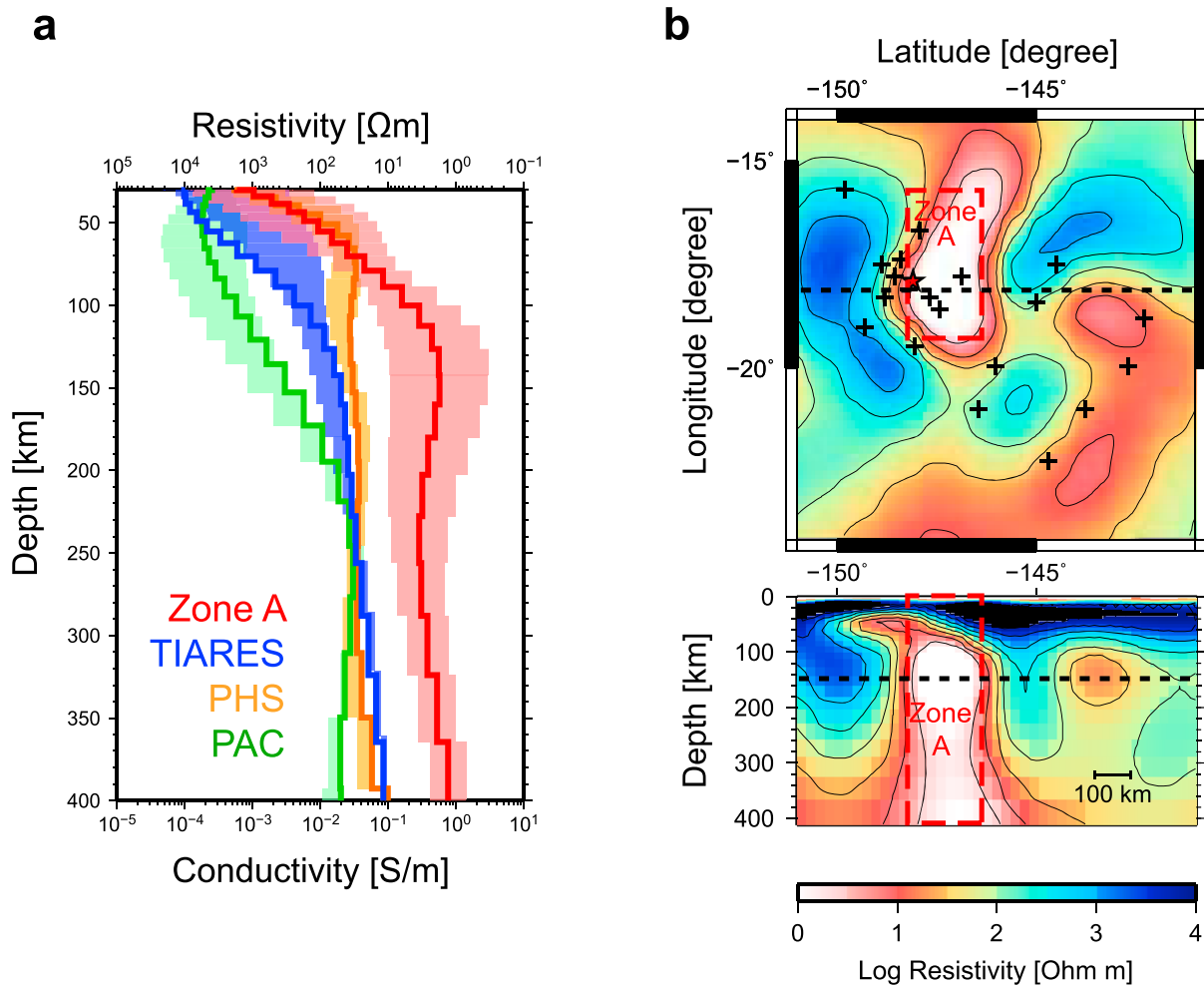


**Figure 2.** Conversion from 3-D model to 1-D electrical conductivity profile. (a) Averaged 1-D electrical conductivities with the standard deviation as a function of depth for Zone A (red). Blue, orange, and green colors denote 1-D electrical conductivity profiles with a plausible area of 70% for the mantle of this study area (the TIARES profile), the Philippine Sea mantle, and the Pacific mantle, respectively. (b) The top panel is a plane view of the 3-D electrical conductivity model at depths of 142–160 km (dashed line in the bottom panel). The bottom panel is a cross-section along the black dashed line in the top panel. Zone A is demarcated by the red dashed line.

shallower than 180 km (Figure 3a). This result indicates that the high conductivity of Zone A is not compatible with a hot and dry mantle model but requires additional conduction mechanism such as effects of partial melting and/or volatiles. Therefore, we use these conductivity profiles to constrain the possible range of melt fraction and H<sub>2</sub>O and CO<sub>2</sub> contents dissolved in the upper mantle rock for Zone A and the whole TIARES study region.

We assume for simplicity that the bulk mantle can be represented by a mixture of olivine and melt. For a given temperature and H<sub>2</sub>O and CO<sub>2</sub> concentrations in the bulk mantle, (However, we assume the hydrogen/carbon (H/C) mass ratio to be either 0.5 or 0.75, which are representative values for oceanic island basalt (OIB) source mantle and mid-ocean ridge basalt source mantle, respectively [Hirschmann and Dasgupta, 2009]), the stable melt fraction and volatile contents in melt and olivine were calculated based on a static model of incipient melting [Hirschmann, 2010]; subsequently, corresponding values of the conductivity of olivine, melt, and bulk mantle were calculated using the results of laboratory experiments [Gardés et al., 2014; Sifré et al., 2014] and a mixing law [Hashin and Shtrikman, 1962] (details provided in Text S3).

For temperature, two profiles were introduced: 1) a typical temperature profile and 2) a higher-temperature profile (higher by 200 °C than the typical profile). The typical temperature profile is estimated by using the plate cooling model [Turcotte and Schubert, 2014] for 70-Ma mantle (black solid line in

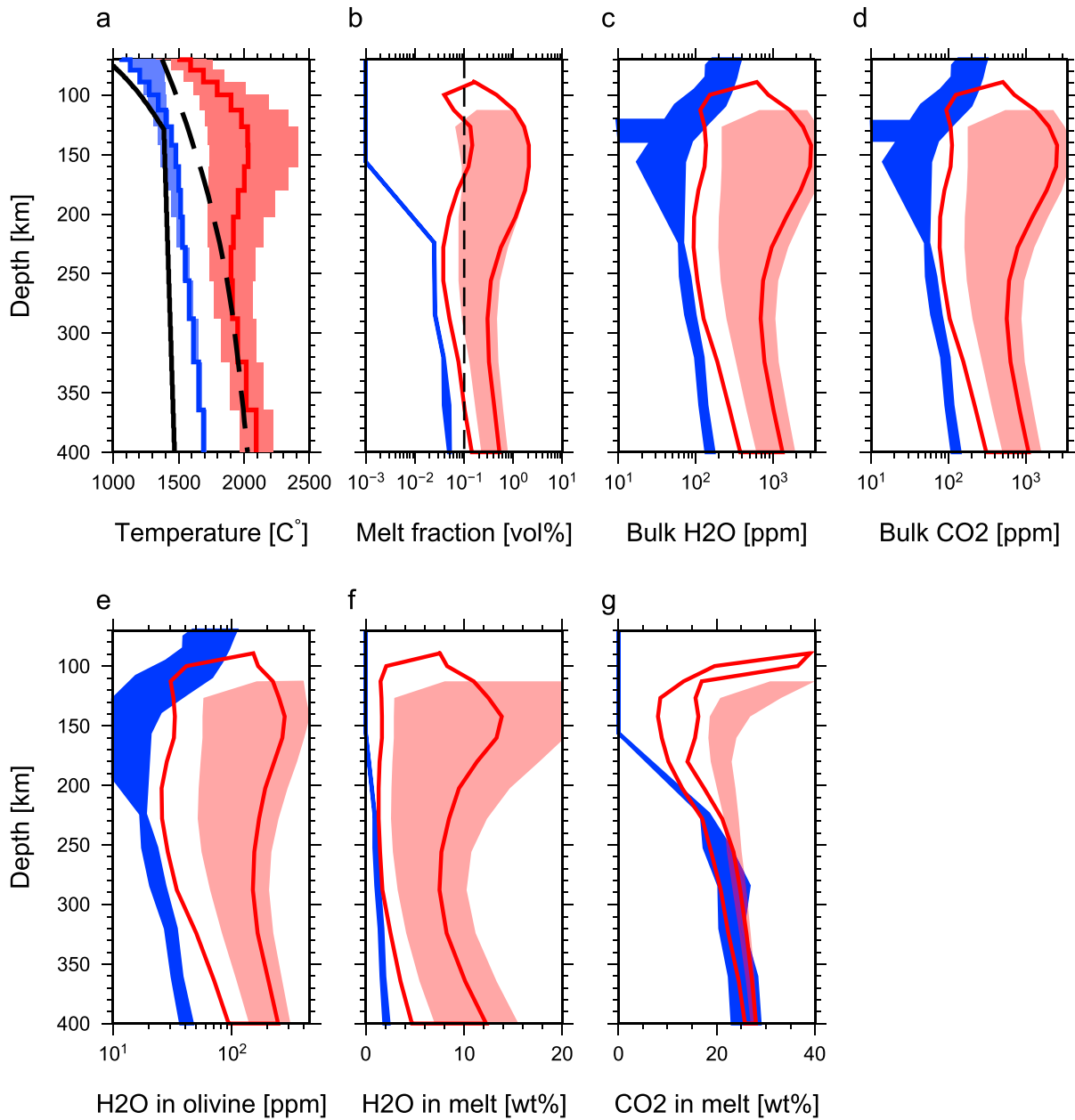


**Figure 3.** Melt fraction and H<sub>2</sub>O and CO<sub>2</sub> contents estimated from the averaged 1-D electrical conductivity profiles assuming OIB source mantle. (a) The temperature profiles as a function of depth for Zone A (red) and the TIARES region (blue) calculated using an empirical law [Gardés *et al.*, 2014] assuming that the upper mantle consists only of dry olivine. The black dashed line denotes the solidus line of dry peridotite [Aubaud *et al.*, 2004]. The black solid line marks the typical temperature profile based on the plate cooling model [Turcotte and Schubert, 2014] for 70 Ma mantle. (b) – (g). Red and blue regions indicate the ranges of each parameter for Zone A and for the TIARES region, respectively, assuming the typical temperature profile. The red solid lines mark the ranges of the estimated values of each parameter for Zone A, assuming that the higher-temperature profile which is the typical temperature plus 200°C.

Figure 3a). The thermal diffusivity is set to be 1 mm<sup>2</sup>/s [Turcotte and Schubert, 2014]. The mantle adiabatic gradient, plate thickness and potential temperature are assumed to be 0.3°C/km, 125 km, and 1350°C, respectively [Baba, 2005].

In terms of 2), we assume that the hotspot is produced by the upwelling of hotter material, as is widely considered to be the case. Suetsugu *et al.* [2009] analyzed seismic receiver functions and concluded that the mantle transition zone (MTZ) beneath the Society hotspot is 150–200°C hotter than the average temperature in the South Pacific which agrees with the global average. Thus, we assumed that the high temperature

anomaly in the MTZ extends to the upper mantle and produced the high-temperature profile by increasing the typical temperature profile by 200 °C.

#### 4. Results and Discussion

The ranges of melt fraction and volatile contents in bulk mantle were determined by comparing modeled and observed 1-D profiles. In case using for the typical temperature profile (the black solid line in Figure 3 a), the upper mantle of the TIARES region doesn't include any melt shallower than at the depth of 160 km. At depths deeper than 160 km, the mantle consists of 60–180 ppmw (parts per million weight) bulk H<sub>2</sub>O (Figure 3c), 50–150 ppmw bulk CO<sub>2</sub> (Figure 3d), and 0.025–0.052 vol.% melt (Figure 3b).

On the other hand, abundant H<sub>2</sub>O and CO<sub>2</sub> are required to account for the high conductivity of Zone A. The upper mantle of Zone A at depths below 100 km is suggested to contain at least 195 ppmw bulk H<sub>2</sub>O (Figure 3c), 160 ppmw bulk CO<sub>2</sub> (Figure 3d), and 0.065–2.2 vol.% melt (Figure 3b). The maximum values of the bulk H<sub>2</sub>O and CO<sub>2</sub> contents are not constrained by the data.

The melt fraction of the upper mantle of Zone A is very well constrained by the data. It is little affected even for the high-temperature profile (Figure 3b). Also, Figure 3g indicates that CO<sub>2</sub> in melt is better constrained by the data, which suggests the presence of carbonated silicate melt in the upper mantle of Zone A. Especially, CO<sub>2</sub> is highly concentrated (around 40 wt.%) in melt at shallower depths (<100 km), which might be caused by reduction in temperature and/or melt fraction. It should be emphasized here that CO<sub>2</sub> is indispensable for explaining the high electrical conductivity of Zone A. A reasonable range of H<sub>2</sub>O (<500 ppmw) alone cannot reproduce the electrical conductivity higher than 0.3 S/m, even assuming the high-temperature profile (Figure S1).

The estimated melt fraction between approximately 120 and 170 km in Zone A is very high, 0.1–2.2 vol.% for any plausible set of parameters. It has been suggested that when the melt fraction exceeds approximately 0.1 vol.%, the melt can migrate upward because of the large buoyancy [Karato, 2014]. Using this idea, the melt fraction obtained appears to be sufficiently large for the melt to move upward rather than stagnating in situ.

The upper mantle of the TIARES region on average shows a signature of rather depleted mantle in terms of H<sub>2</sub>O and CO<sub>2</sub> compared to that of Zone A. For the TIARES region, the temperature profile converted from the conductivity profile under the assumption of dry condition agrees well with the typical temperature profile at depths shallower than 180 km and is lower than the solidus of dry olivine (Figure 3a). These signatures imply that neither melt, hydrogen, nor carbon is abundant in the upper mantle of the TIARES region on average in the depth range. Furthermore, the contrast between the TIARES region and Zone A suggests that the chemical contamination of the ambient mantle by plume occurs in very limited zone.

#### 5. Conclusions

We conducted a seafloor magnetotelluric survey around the Society hotspot and obtained the first image of three-dimensional high electrical conductivity anomaly in the upper mantle beneath the Society hotspot. This anomaly seems to be continuous from the lowest part of the upper mantle to a depth of approximately 50 km below sea level, which is one to two orders of magnitude higher than even the younger upper mantle beneath the Philippine Sea. The electrical conductivity of the background region is not anomalous in terms of age-dependence.

The high electrical conductivity anomaly is interpreted to be caused by an upper-mantle melt fraction up to 2.2 vol.%, which is robust regardless of temperature. The existence of carbonated silicate melt in the upper mantle beneath the Society hotspot is confirmed because of CO<sub>2</sub> in the melt is well constrained to be at least 8 wt.%. The features of the anomaly strongly suggest the upwelling of volatile-rich, partially molten material in the upper mantle beneath the hotspot. Our observations may place constraints on the scale and role of both upper mantle convection and carbon flux related to the mantle plume.

#### References

- Adam, C. (2005), Extent of the South Pacific Superswell, *J. Geophys. Res.*, 110, B09408, doi:10.1029/2004JB003465.
- Adam, C., M. Yoshida, T. Isse, D. Suetsugu, Y. Fukao, and G. Barruol (2010), South Pacific hotspot swells dynamically supported by mantle flows, *Geophys. Res. Lett.*, 37, L08302, doi:10.1029/2010GL042534.

#### Acknowledgments

We thank the scientific party, captain, crews of RV *Mirai* and the Tahitian fishing boat *Fetu Mana* for work that made this study possible. We thank D. Reymond, P. Mery and J.-P. Barriot for their support in Tahiti. We would like to thank editor A. V. Newman and anonymous reviewers for providing valuable comments, which were useful to significantly improve the manuscript. Institut national des sciences de l'univers (INSU) – Centre national de la recherche scientifique (CNRS) funded the marine operation with Division Technique de l'INSU and J. F. D'Eu from CNRS. This work was partially supported by JSPS KAKENHI grant JP19253004, JP23740346, and JP15H03720. OBEM data from the TIARES project are open to the public on the Pacific21 website (<http://p21.jamstec.go.jp/top/>). We have used the computer systems of the Earthquake and Volcano Information Center of the Earthquake Research Institute, the University of Tokyo, and have used the SC system of Japan Agency for Marine-Earth Science and Technology. The GMT software package [Wessel and Smith, 1998] was used in the present study.

- Amente, C., B. W. Eakins (2009), ETOPO1 1 arc-minute global relief model: Procedures, data sources and analysis, 19 pp., NOAA Tech. Memo. NEDIS NGDC-24. Natl. Geophys. Data Center, Mar. Geol. and Geophys. Division, Boulder, Colo.
- Aubaud, C., E. Hauri, and M. M. Hirschmann (2004), Hydrogen partition coefficients between nominally anhydrous minerals and basaltic melts, *Geophys. Res. Lett.*, *31*, L20611, doi:10.1029/2004GL021341.
- Aubaud, C., F. Pineau, R. Hekinian, and M. Javoy (2005), Degassing of CO<sub>2</sub> and H<sub>2</sub>O in submarine lavas from the Society hotspot, *Earth Planet. Sci. Lett.*, *235*(3-4), 511–527, doi:10.1016/j.epsl.2005.04.047.
- Baba, K. (2005), Electrical Structure in Marine Tectonic Settings, *Surv. Geophys.*, *26*(6), 701–731, doi:10.1007/s10712-005-1831-2.
- Baba, K., and A. D. Chave (2005), Correction of seafloor magnetotelluric data for topographic effects during inversion, *J. Geophys. Res.*, *110*, B12105, doi:10.1029/2004JB003463.
- Baba, K., H. Utada, T. Goto, T. Kasaya, H. Shimizu, and N. Tada (2010), Electrical conductivity imaging of the Philippine Sea upper mantle using seafloor magnetotelluric data, *Phys. Earth Planet. Inter.*, *183*(1-2), 44–62, doi:10.1016/j.pepi.2010.09.010.
- Baba, K., N. Tada, H. Utada, and W. Siripunvaraporn (2013), Practical incorporation of local and regional topography in three-dimensional inversion of deep ocean magnetotelluric data, *Geophys. J. Int.*, *194*(1), 348–361, doi:10.1093/gji/ggt115.
- Chave, A. D., and D. J. Thomson (2004), Bounded influence magnetotelluric response function estimation, *Geophys. J. Int.*, *157*(3), 988–1006, doi:10.1111/j.1365-246X.2004.02203.x.
- Duncan, R. A., and I. McDougall (1976), Linear Volcanism in French Polynesia, *J. Volcanol. Geotherm. Res.*, *1*(3), 197–227, doi:10.1016/0377-0273(76)90008-1.
- Gardés, E., F. Gaillard, and P. Tarits (2014), Toward a unified hydrous olivine electrical conductivity law, *Geochem. Geophys. Geosyst.*, *15*, 4984–5000, doi:10.1002/2014gc005496.
- Hashin, Z., and S. Shtrikman (1962), A Variational Approach to Theory of Effective Magnetic Permeability of Multiphase Materials, *J. Appl. Phys.*, *33*(10), 3125–3131, doi:10.1063/1.1728579.
- Hirschmann, M. M. (2010), Partial melt in the oceanic low velocity zone, *Phys. Earth Planet. Inter.*, *179*(1-2), 60–71, doi:10.1016/j.pepi.2009.12.003.
- Hirschmann, M. M., and R. Dasgupta (2009), The H/C ratios of Earth's near-surface and deep reservoirs, and consequences for deep Earth volatile cycles, *Chem. Geol.*, *262*(1-2), 4–16, doi:10.1016/j.chemgeo.2009.02.008.
- Isse, T., H. Sugioka, A. Ito, H. Shiobara, D. Reymond, and D. Suetsugu (2016), Upper mantle structure beneath the Society hotspot and surrounding region using broadband data from ocean floor and islands, *Earth Planets Space*, *68*, 33, doi:10.1186/s40623-016-0408-2.
- Karato, S.-I. (2014), Does partial melting explain geophysical anomalies?, *Phys. Earth Planet. Inter.*, *228*, 300–306, doi:10.1016/j.pepi.2013.08.006.
- Nolasco, R., P. Tarits, J. H. Filloux, and A. Chave (1998), Magnetotelluric imaging of the Society Islands hotspot, *J. Geophys. Res.*, *103*, 30,287–30,309, doi:10.1029/98JB02129.
- Sifré, D., E. Gardés, M. Massuyeau, L. Hashim, S. Hier-Majumder, and F. Gaillard (2014), Electrical conductivity during incipient melting in the oceanic low-velocity zone, *Nature*, *509*(7498), 81–85, doi:10.1038/nature13245.
- Suetsugu, D., T. Isse, S. Tanaka, M. Obayashi, H. Shiobara, H. Sugioka, T. Kanazawa, Y. Fukao, G. Barruol, and D. Reymond (2009), South Pacific mantle plumes imaged by seismic observation on islands and seafloor, *Geochem. Geophys. Geosyst.*, *10*, Q11014, doi:10.1029/2009GC002533.
- Suetsugu, D., et al. (2012), TIARES Project—Tomographic investigation by seafloor array experiment for the Society hotspot, *Earth Planets Space*, *64*(4), i–iv, doi:10.5047/eps.2011.11.002.
- Tada, N., K. Baba, W. Siripunvaraporn, M. Uyeshima, and H. Utada (2012), Approximate treatment of seafloor topographic effects in three-dimensional marine magnetotelluric inversion, *Earth Planets Space*, *64*(11), 1005–1021, doi:10.5047/eps.2012.04.005.
- Turcotte, D. L., and G. Schubert (2014), *Geodynamics*, 3rd ed., Cambridge Univ. Press, Cambridge.
- Wessel, P., and W. H. F. Smith (1998), New, improved version of the generic mapping tools released, *Eos Trans. AGU*, *79*, 579, doi:10.1029/98EO00426.